Direct Observation of Growth of Lamellae and Spherulites of a Semicrystalline Polymer by AFM

Lin Li,† Chi-Ming Chan,* King Lun Yeung, Jian-Xiong Li, Kai-Mo Ng, and Yuguo Lei

Department of Chemical Engineering, Advanced Engineering Materials Facility, Hong Kong University of Science and Technology, Clear Water Bay, Hong Kong

Received February 14, 2000; Revised Manuscript Received October 31, 2000

ABSTRACT: The dynamic growth processes of lamellae and spherulites of a polymer (BA-C8) synthesized by condensation polymerization of bisphenol A and 1,8-dibromooctane were directly observed using an atomic force microscope at 25 ± 1 °C. The phase shift measured at the tip of growing lamellae is lower than the phase shifts of the other regions of the lamellae. This result indicates that the growth front of a lamella is softer and contains more defects than the developed ones. The growth process of lamellae and the formation of spherulites were studied. A lamella was observed to breed more lamellae by inducing adjacent secondary nuclei and to develop into a lamellar sheaf and finally into a spherulite. The lamellae were preferentially oriented edge-on with respect to the surface of the BA-C8 polymer thin films. The detailed observations on the formation of the secondary nuclei indicated that the branching of the lamellae was only a temporary growth stage of the secondary lamellae. At the branch point, the secondary lamellae could propagate in both backward and forward directions with respect to the growth direction of the parent lamellae.

Introduction

When a polymer crystallizes from the melt without disturbance, it normally forms spherical structures that are called "spherulites".[1,2] The dimensions of spherulites range from micrometers to millimeters, depending on the structure of the polymer chain and the crystallization conditions, such as cooling rate, crystallization temperature, and the content of the nucleating agent. The structure of spherulites is similar regardless of their size; they are aggregates of crystallites.[1−6]

Much effort has been devoted to investigating the detailed architectures and construction of spherulites. The early investigations of the crystallization of polymers through optical microscopy[7,8] posited that that polymer spherulites consisted of radiating fibrous crystals with dense branches to fill space. Later, when electron microscopy became available, spherulites were shown to be comprised of layerlike crystallites,[9,10] which were named lamellae. The lamellae are separated by disordered materials. In the center of the spherulites, the lamellae are stacked almost in parallel.[5,6,11−15] Away from the center, the stacked lamellae splay apart and branch, forming a sheaflike structure.[11,13−15] It was also found that the thicknesses of lamellae are different.[5,6,11,12] The thicker ones are believed to be primary lamellae while the thinner ones are secondary lamellae.

Electron microscopy is suitable for examining only the static structures of materials and cannot been used to observe the growth process of spherulites. Examining the internal structure of growing spherulites in a partially crystallized and quenched polymer sample overcomes this drawback to a certain extent, and the process of spherulite formation has been deduced.[4,6,11] A spherulite is believed to develop from a stack of lamellae. During the growth process, the stacked lamellae splay apart continually and branch occasionally. The continuous growth of the primary lamellae forms a spherical skeleton, and the secondary lamellae fill up the space between the primary lamellae. But this process is still hypothetical because the description is not based on direct observations of the formation of spherulites. Furthermore, how the stacked lamellae are generated is still not clear, though nucleation of a supercooled melt can be predicted from thermodynamics,[4] and both small-angle X-ray and wide-angle X-ray diffraction experiments using synchrotron radiation indicted that polymers must undergo spinodal decomposition before crystallites are detectable.[4,16,17]

Splaying apart and branching of lamellae to form spherulites due to the repulsion of the amorphous materials between the lamellae are the general features of polymer spherulites.[4,11,14,15] It is understood that to achieve a spherical shape, primary lamellae have to splay apart and branch. Even so, the origins for the splaying and branching processes have not been confirmed. The early investigations of polymer crystallization suggested that the accumulation of noncrystallizable impurities in the front of growing lamellae was the reason for branching.[18] But several authors have queried this diffusion-control mechanism. On the basis of the morphology of growing spherulites in quenched samples, Bassett and colleagues proposed that branching is a result of secondary nucleation on primary lamellae.[11] They also suggested that the mutual repulsion between the adjacent primary lamellae, resulting from the protruding "cilia" of the lamellae, is the origin for splaying of the stacked lamellae. However, the secondary nucleation and splaying processes have never been observed directly owing to the limitations of electron microscopy.

The invention of atomic force microscopy (AFM)[19−23] has made direct observation of the crystallization of polymers possible. In addition to its high resolution,

* To whom correspondence should be addressed.
† Present address: State Key Laboratory of Polymer Physics and Chemistry, Center for Molecular Science, Institute of Chemistry, Chinese Academy of Science, Beijing China, 100080.

10.1021/ma000273e CCC: $20.00
Published on Web 12/19/2000

Scheme 1. Synthesis of BA-C8 Polymer

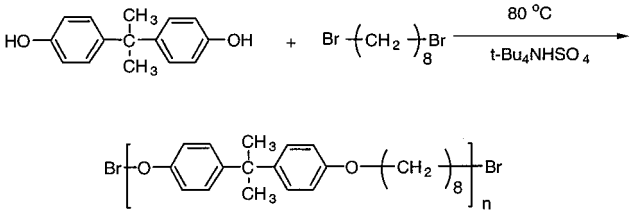

contact-mode AFM can record real-time images of a dynamic process. The disadvantage of contact-mode AFM is the considerable pressure exerted by the probe tip on the sample surface, causing sample deformation. In particular, such damage to soft samples such as polymers and biological specimens limits the applicability of AFM. In recent years, the development of tapping-mode AFM (TM-AFM) has enhanced the capability of AFM as a surface analysis technique.[22,23] In TM-AFM, a fast oscillating probe is used for surface imaging. During the operation, the tip makes contact with the surface briefly in each cycle of oscillation. Many studies have been performed to interpret the height and phase images recorded by TM-AFM.[24−27] Results clearly indicate that phase images can provide enhanced contrast on heterogeneous surfaces. TM-AFM has been shown to be a powerful tool to study the surfaces of polymer blends, copolymers, and semicrystalline polymers.[22,24,25,28−31]

By utilizing the advantages of AFM, the spherulites and lamellae of various semicrystalline polymers have been investigated.[32−47] The lamellar thickness[36,48] and hedritic morphology[41] of polypropylene were studied by Vancso and colleagues, and the thickness of the lamellae was found to be identical to the values in the literature as revealed by other techniques. The growth rates of a spherulite and the internal lamellae of a poly(hydroxybutyrate-*co*-valerate) copolymer have been determined by Barham and colleagues with TM-AFM.[45] The result indicated that the overall gross growing front of a spherulite can propagate at a constant rate, but the internal lamellae cannot. It was believed that the spherulite growth rate is dependent on the rate of secondary nucleation on the existing lamellae but not on the growth rate of the lamellae. Melting and crystallization of poly(ethylene oxide),[34,44] poly(ethylene oxide) in poly(ethylene oxide)/poly(methyl methacrylate) blends,[35] poly(ether ether ketone),[40] and polyethylene[42] have been studied by an AFM equipped with a hot stage.

The crystallization rate and crystallinity of a polymer are strongly dependent on the crystallization temperature and the polymer chain structure.[49] For poly(bisphenol A alkyl ether), the crystallization rate can be adjusted by changing the length of the flexible alkyl segment.[50] In this study, a series of poly(bisphenol A alkyl ether) with various flexible segments have been synthesized. Under ambient conditions, poly(bisphenol A octane ether) (BA-C8) crystallizes at a rate that is suitable for AFM to map the crystallization process without a hot stage. This allows direct observation of the whole crystallization process from the generation of the nuclei to the growth and development of lamellae to the formation of spherulites. In this paper, the growth of lamellae and the formation of spherulites are described.

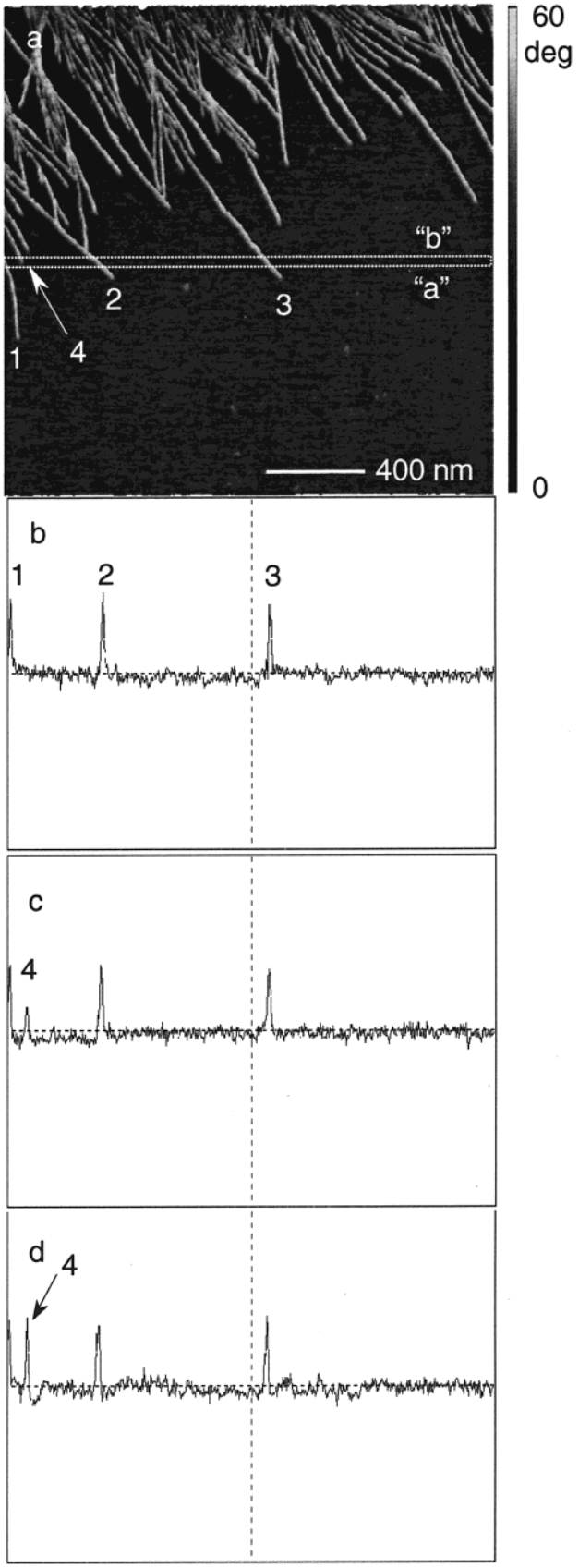

Figure 1. AFM observations of the tips of growing lamellae: (a) AFM phase images. (b), (c), and (d) are the retraced phase signals between the two dotted lines a and b, as shown in Figure 2a.

Experimental Section

A poly(bisphenol A octane ether) (BA-C8) was synthesized by condensation polymerization of bisphenol A and 1,8-dibromoctane. The glass transition temperature, melting point, number-average molecular weights (M_w), and polydispersity indices ($\bar{M}_w/\bar{M}_n$) of the polymer were measured to be 6.3 °C,

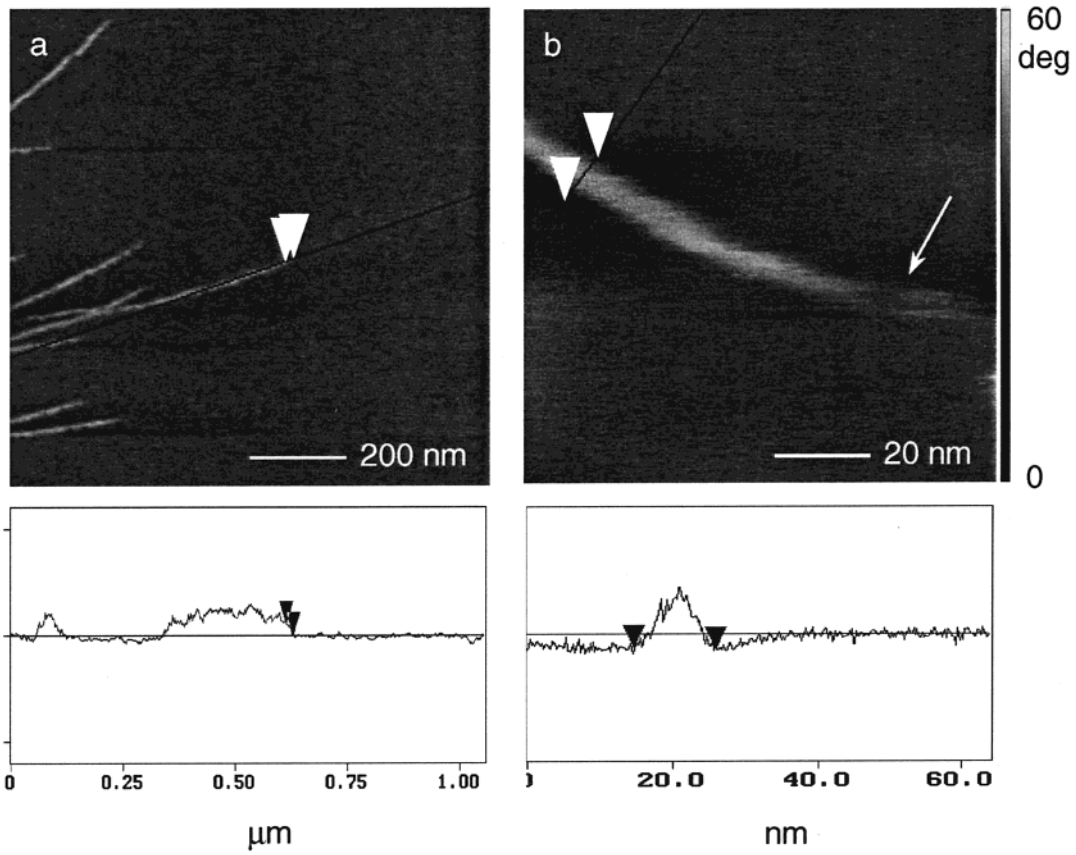

Figure 2. Measurements of the length of a growing lamellar tip and the thickness of a lamella using AFM: (a) the length of the imperfect region of a lamellar tip and (b) the thickness of a lamella.

84.3 °C, 9500 g/mol, and 1.68. The synthesis scheme is described in Scheme 1. Thin BA-C8 polymer films were prepared by spin-coating a 30 mg mL^{-1} polymer−chloroform solution onto a silicon wafer surface (∼10 mm × 10 mm) at 3000 rpm. The samples were dried in a vacuum at 25 ± 1 °C for 15 min. The thickness of the amorphous BA-C8 film was estimated to be approximately 300 nm by using a profilometer.

Tapping mode AFM images were obtained at ambient conditions using a NanoScope III MultiMode AFM (Digital Instruments). Both height and phase images were recorded simultaneously using the retrace signal. Si tips with a resonance frequency of approximately 300 kHz and a spring constant of about 40 N m^{-1} were used, and the scan rate was in the range 0.5−1.2 Hz. The scanning density was 512 lines/frame, and the amplitude of the free-oscillating cantilever was approximately 40 nm. The amplitude set ratio of 0.72 was used unless specified. The phase contrast imaging technique was employed to distinguish the amorphous phase from the crystalline phase. When the oscillating AFM probe is scanned along the surface, the soft amorphous material is more compliant than the harder crystalline material. This results in a phase difference between the soft and hard materials, thus providing a distinct contrast between the two phases.

Results and Discussion

Lamellar Growth and Secondary Nucleation. Figure 1 shows highly magnified AFM images of lamellae at the growth front of a spherulite of a BA-C8 polymer thin film. Figure 1a is an AFM phase image of edge-on lamellae. Most of the lamellae are seen edge-on with respect to the substrate, and flat-on lamellae are seen only at the eyes of the spherulites. Godovsky and Magonov also observed mostly edge-on lamellae on an unltrathin low-density polyethylene film on silicon substrate.[42] It is possible that the edge-on lamellae form a more stable interface with the substrate. Figure 1b−d shows the retrace phase signals obtained between the two dotted lines a and b, as shown in Figure 1a. The dotted line a crosses the developed portions of lamellae 1, 2, and 3. The corresponding retrace phase signal obtained close to line a is shown in Figure 1b. It can be seen that the retrace phase signals at the developed portion of the three lamellae are similar.

Figure 1c shows the retrace phase signal obtained along a line between lines a and b. Now, the tracing line crosses not only lamellae 1, 2, and 3 but also the tip of lamella 4 as well. The phase shift at the tip of lamella 4 is evidently lower than the shifts at lamellae 1, 2, and 3. This indicates that the growth front of a lamella is softer and contains more defects than the developed ones. Figure 1d shows the retrace phase signal along a line very close to line b. This line crosses the developed portions of all four lamellae. It can be seen that the phase shifts for the four lamellae are more or less identical. This figure further indicates that the developed regions of the lamellae contain fewer defects. Using the retrace phase signals along growing lamellae, the length of the lamellar tips was estimated to be 5−20 nm, as shown in Figure 2a. Similarly, the thickness of an "edge-on" lamella was measured to be approximately 10 nm, as shown in Figure 2b. It is important to point out that these measurements could be affected by the tip−surface convolution effect when the size of the tip (∼20 nm) is similar to that of the measured objects.[41] Compared with the thickness of the lamellae, the length of the lamellar tips is rather long. This observation seems to indicate that the growing front of the lamellae is highly ordered and the irregular conformation (defects) in the growth front of the lamellae moves out from

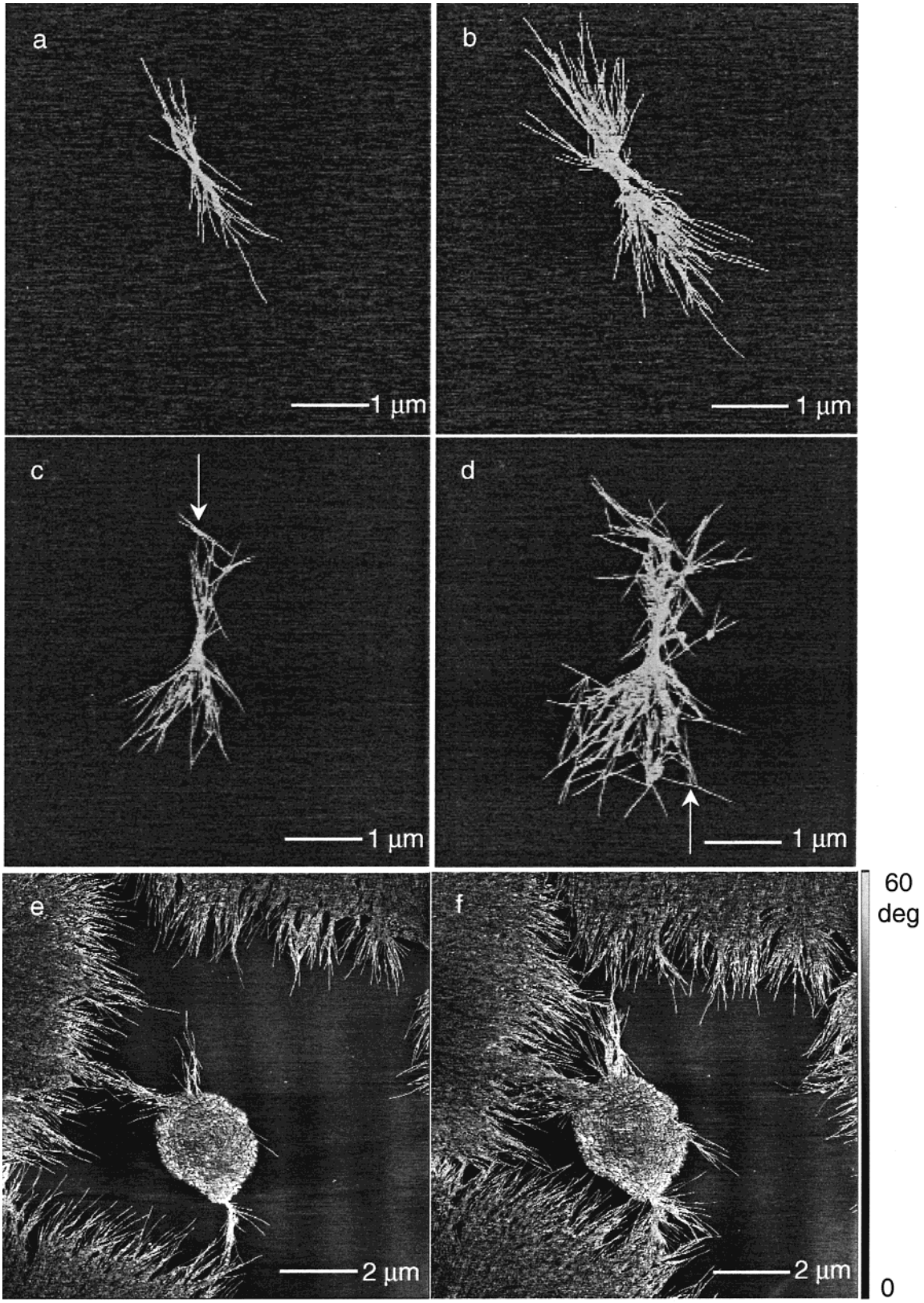

Figure 3. AFM phase images showing the influence of the AFM probe on the growth direction of lamellar tips: (a) and (b) set point amplitude ratio of 0.72; (c) and (d) set point amplitude ratio of 0.60; and (e) and (f) set point amplitude ratio of 0.44.

the tip gradually as the lamellae propagate. This proposed structure for the lamellar tip qualitatively agree with the model proposed by Strobl.[51] In his model, a lamellar tip is a mesomorphic layer which is composed of imperfectly stretched sequences in a liquidlike cylinder packing.

The chain segments in the tips of the growing lamellae are not packed as well as those in the developed regions of the lamellae. It is of interest to investigate the effect of pressure induced by an AFM tip on the growth of the lamellae. When the set point amplitude ratio decreases, the pressure exerted on the surface by

the AFM probe increases. For example, Figure 3 shows a series of AFM images obtained at different set point amplitude ratios. Figure 3a,b was obtained at the set point amplitude ratio of 0.72. At this position, the influence of the AFM probe on the propagation of the growing lamellae is small. A primary lamella breeds more lamellae and develops into a lamellar sheaf. When the set point amplitude ratio is decreased to 0.60, the growth direction of some of the lamellae changes, as illustrated by the arrow in Figure 3c. More lamellae are forced to change their growth directions during the sequential AFM scanning of the same area, as shown in Figure 3d. When the set point amplitude ratio is reduced further to 0.44, the effect of the AMF tip on the propagation of lamellae becomes more significant, as shown in Figure 3e,f. An edge-on lamella changes into a flat-on lamella. However, when the set point amplitude ratio is changed back to 0.72, the growth of edge-on lamellae resumed due to the restraint in the growth direction of the flat-on lamellae. At this point, it unclear to us that why pressure can cause such changes.

When the AFM probe is operated at the set point amplitude of 0.72, the disturbance caused by the oscillating AFM probe to the growing tip of the "edge-on" lamellae is relatively small. The BA-C8 chain segments fit into the lattice of the "edge-on" lamellae along their growth directions. However, when the set point amplitude ratio is decreased to 0.60, the imperfect orientation of the BA-C8 chain segments of the growing tips is disturbed, and the growth direction of the "edge-on" lamellae is changed, as shown in Figure 3c,d. When the set point amplitude ratio is further decreased to 0.44, an "edge-on" lamella changes to a "flat-on" lamella, because the "*a*−*b*" plane of a lamella should be more stable to the disturbance based on the geometrical argument. The change from an "edge-on" lamella to a "flat-on" lamella is induced by the high pressure exerted by the AFM probe.

Figure 4 shows a sequence of AFM images of the lamellae at the growth front of a spherulite. The time interval between each consecutive image is approximately 9 min. The left column of Figure 4 displays the AFM topographic images, and the right column shows the corresponding phase images. The data scales of the AFM height images are 15 nm in Figure 4a−c and 25 nm in Figure 4d,e. As shown in the height image, the surface of the BA-C8 thin film becomes rough as random chain segments accommodate themselves into the lattice as the lamellae propagate. Individual lamella can be seen clearly in the phase image (right column of Figure 4). The lamellae in the front of a spherulite do not grow at a constant rate. A lamella can propagate with various speeds at different times and locations (cf. lamellae 1 and 2 in Figure 4). At the beginning of this series of images, lamella 2 is behind lamella 1. But later as the growth rate of lamella 2 increases (cf. Figure 4c,d), lamella 2 surpasses lamella1 (cf. Figure 4d). A similar phenomenon was observed in a film of poly(hydroxybutyrate-*co*-valerate) copolymer.[45]

Secondary nuclei are observed to form near or at dominant lamellae by TM-AFM phase imaging. Normally, the secondary nuclei appear at a location of 0.5−1.0 μm behind the tip of growing lamellae, as shown in Figure 4a,b. It can be seen that lamella 1 induces a secondary nucleus. On further growth, the secondary nucleus develops into branches. More interestingly, the

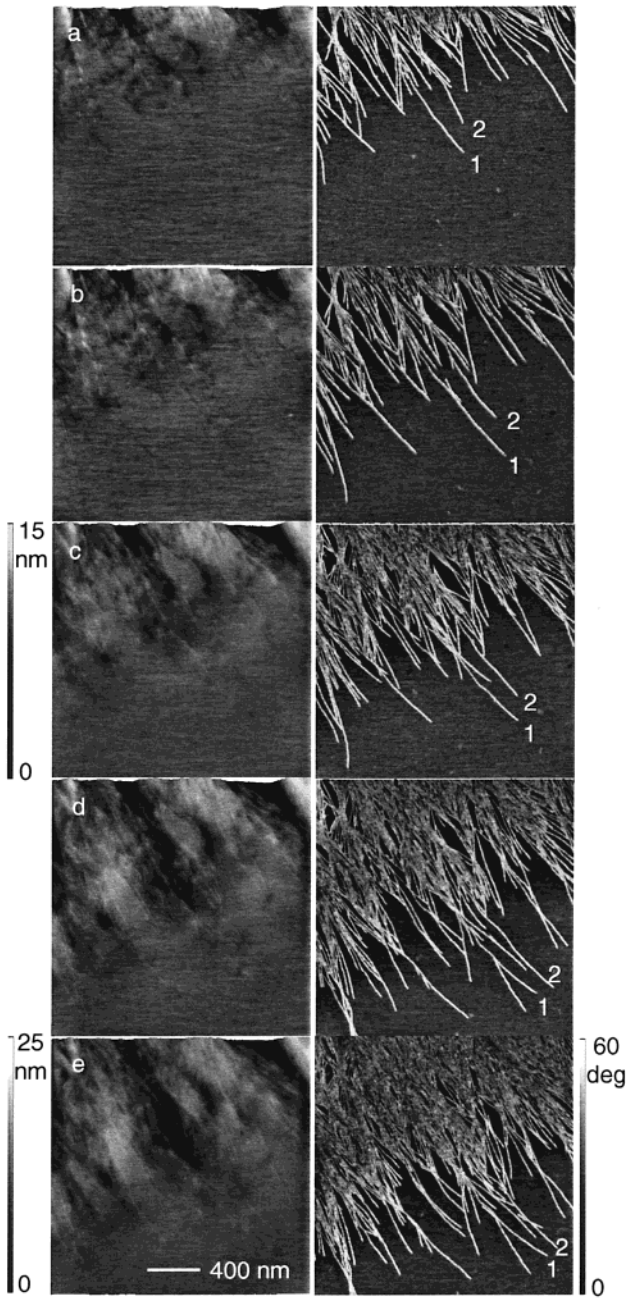

Figure 4. A series of images of the growth front of a spherulite in a consecutive time sequence.

secondary lamella grows away from the secondary nucleus site in either or both forward and backward directions. Furthermore, the secondary lamellae can also induce secondary nucleation. In this way, the primary lamellae induce many branches in a spherulite. The above results provide direct evidence for Bassett's suggestion that the branching of lamellae might result from secondary nucleation on the primary lamellae.[11]

However, the above results do not suggest that secondary nucleation is the sole origin of branching of lamellae. Branching can also occur when two lamellae are joined together. Figure 5a−d is an enlarged view (software zooms) of the lamellae shown in Figure 4b−e, revealing a detailed picture of propagation and branching of lamellae. The joining sites of the lamellae are labeled as J1, J2, and J3. The joining of two propagating lamellae can occur at the tips. As shown in Figure 5a,b, the two tips of the growing lamellae

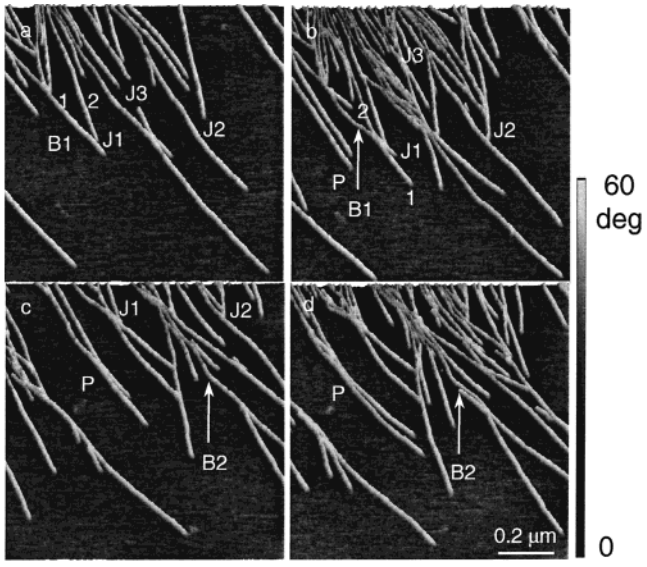

Figure 5. Joining and bending of lamellae during their growth and propagation.

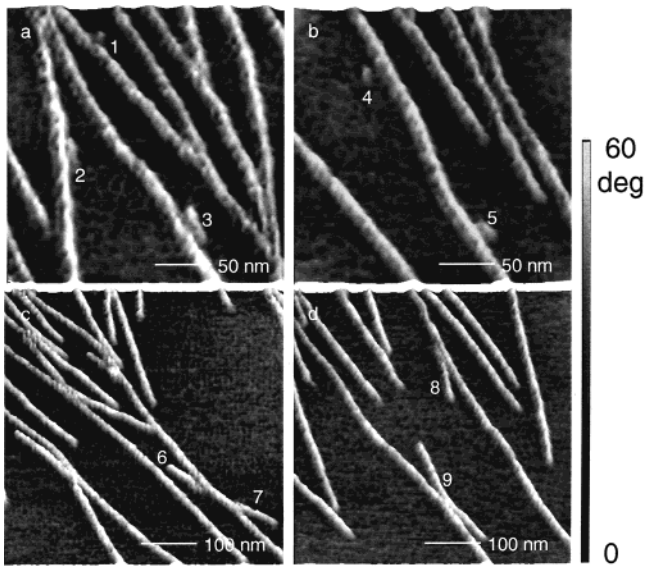

Figure 6. AFM phase images showing the secondary nuclei and secondary "edge-on" lamellae.

approach each other and join together. After joining, the growth of the lamellae might resume again (cf. J1 in Figure 5c). Also, the joining of lamellae can occur between the tips of a growing lamella and an existing lamella (cf. J2 in Figure 5a,b). In this case, joining might lead to a termination of growth of the lamella whose tip joins with the other lamella (cf. J2 in Figure 5b,c). Additionally, when a forward growing lamella meets a backward growing lamella developed from a secondary nucleus (cf. J3 in Figure 5a), the opposing lamellae can join together (cf. J3 in Figure 5b). One very interesting observation is seeing the joining of two lamellae initially propagating parallel to one another (cf. P in Figure 5b). After the parallel growth of the two lamellae lasts for about 1.0 μm, the two lamellae begin to come closer and closer and finally join together (cf. P in Figure 5c). After joining, the two lamellae could separate and propagate again (cf. P in Figure 5d). The tension of the molecular chains trapped between the parallel lamellae is believed to cause the joining of the two lamellae. As the chain segments fit into the lattice of the lamellae, they might pull the two lamellae together.

Another interesting phenomena observed here is that joining might cause a bending of lamellae. In Figure 5a, lamella 1 is propagating along a straight line. As lamella 2 joins with lamella 1 at the location marked B1, lamella 1 becomes bowlike. More surprising, bending can also occur when a lamella passes by another lamella as marked as B2 in Figure 5. When a daughter lamella grows close to a mother lamella, the mother lamella bended toward the daughter lamella.

Secondary nucleation is also investigated at a high magnification (cf. Figure 6, a software zoom of Figure 5). Secondary nuclei are generated close to existing lamellae. Some are formed at a short distance away from their mother lamellae while others are in contact with their mother lamellae (cf. nuclei 1−5 in Figure 6). Compared with the primary nuclei, secondary nuclei are relatively stable. Once they are formed, they usually grow continuously into secondary lamellae without disintegration. As the secondary nuclei grow, the gap between the mother and daughter lamellae may diminish and even disappear (cf. lamellae 6 and 7 in Figure 6).

A macromolecule chain prefers to stay as a random coil. Under supercooling, an ordered embryo of a crystallite may form within the random coils by adjusting the conformation of their chain segments through molecular thermal motion. When the embryo is large enough, it becomes stable and grows continuously. The lamellae grow by having the nearby chain segments adjusting their conformations and accommodate themselves into the lattice of the existing lamellae.[4] Compared with the thickness of lamellae, the random coils are much larger.[52] There is certainly some mass migration during crystallization. This observation is supported by the fact that the surface of the film becomes rough as crystallization proceeds (cf. Figure 4). However, long-distance migration of the polymer chains is not favorable because of high viscosity and physical entanglements. Consequently, the two faces ($a-b$ planes) of a lamella should consist of a high concentration of loose loops or protruding cilia of the polymer chains.[11,52] When one end of these polymer chains is trapped in the lamellae, the mobility of these polymer chains decreases. Hence, there is a higher probability for them to line up in more orderly fashion, forming secondary nuclei close to the mother lamellae. This can explain why all experimental observations show that secondary nuclei are located close to the parent lamellae. Also, because it will take time for the protruding chain segments to change their orientations or adjust their conformations, secondary nuclei are usually generated after the mother lamellae have propagated for a certain distance (about 1 μm). This may also explain why that when two growing lamellae meet, their growth rates could be significantly reduced. After the secondary nuclei have formed, they can grow away from the nucleation sites in either or both the forward and backward directions, depending on the lattice orientation and the availability of polymer materials. However, in the backward direction, the supply of materials is limited because most of the polymer chains have been trapped by the adjacent lamellae. Hence, the fitting of the chain segments into the lattice of the daughter lamellae will take longer. This is the reason why secondary lamellae grow more slowly in the backward direction.

Even for the protruding lamellae, the original orientation of the chain segment near the tips of the growing

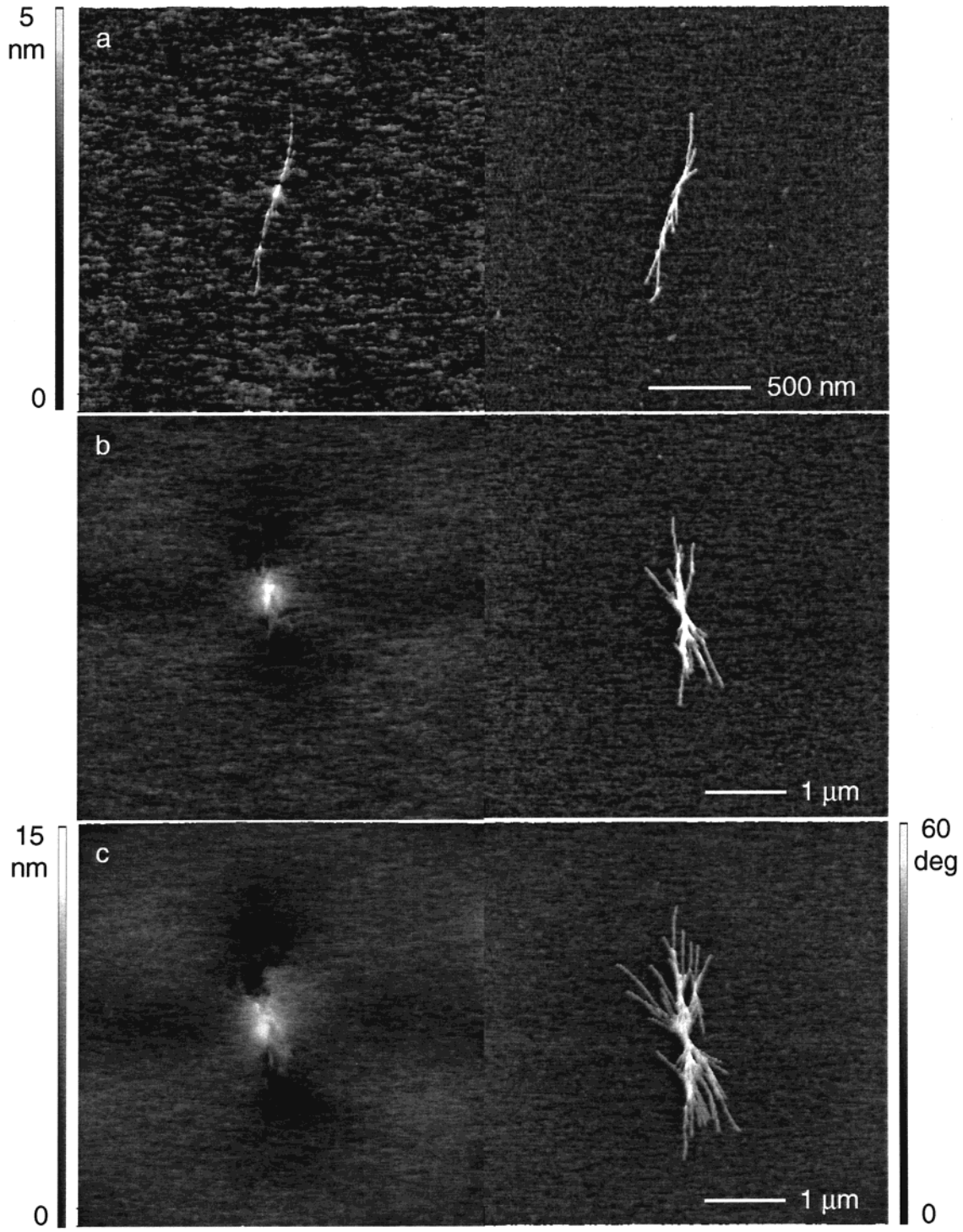

Figure 7. Development of a lamellar sheaf: (a) lamellae are bred from a single nucleus; (b) the lamellae splaying apart and breeding more lamellae; and (c) formation of a lamellar sheaf.

lamellae may be different at different locations. They may take different lengths of time to adjust their conformations to fit themselves into the lattice of the lamellae. Therefore, the lamellae do not propagate at a constant rate but a variable rate that changes with location. When two lamellae propagate parallel and very close to each other, their growth rates and directions may be affected by the original orientation of the chain segments near the tip of the growing lamellae. A newly formed lamella usually does not assume a perfect order. The defects may diffuse out of the lamellar tip continuously. If a daughter lamella has the same lattice orientation as its mother lamella and the materials at the gap between them do not contain any structural defects, the daughter lamella can joint with the mother lamella. In the same way, a growing lamellae can joint with an existing lamella, provided that the majority of the mismatched structures are removed from their growth paths. However, we should point out that the join between the lamellae is not defect-free. It is highly possible that defects in the join are more severe than in the lamellae themselves.

Spherulite Development. The whole process of formation of spherulites was clearly observed under TM-AFM clearly. Figures 7 and 8 present the observed results. The left and right columns of Figure 7 display

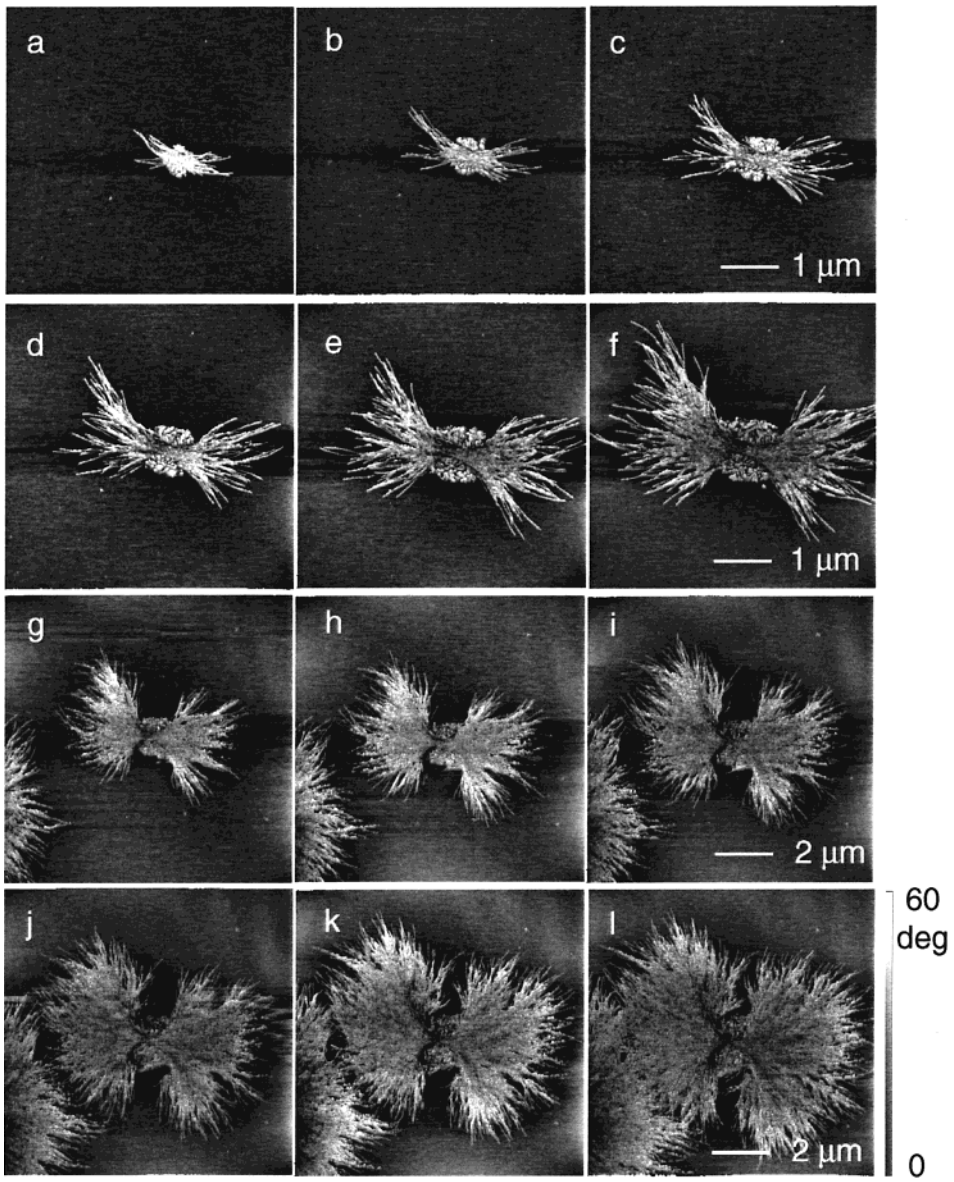

Figure 8. A series of AFM images showing the formation of a spherulite.

the topographic images and the corresponding AFM phase images, respectively. The data scales of the AFM height images are 5 nm in Figure 7a and 15 nm in Figure 7b,c. As seen from Figure 7a, in the early stage of growth, a single lamella breeds more lamellae and develops into an embryo of a spherulite. As the primary lamellae grow at the two ends, they splay apart from each other. Meanwhile, they breed more lamellae through secondary nucleation. As a result of this continuous growing, splaying, and breeding secondary lamellae, the initial lamellae gradually evolve into a lamellar sheaf, as shown in Figure 7b,c.

Figure 8 shows the process of a lamellar sheaf developing into a spherulite skeleton upon further growth of the lamellae. Through continuous splaying and secondary nucleation, the edge-on lamellae spread gradually across the film to form a spherulite. The process of formation of spherulites observed by TM-AFM is consistent with that proposed on the basis of the morphologies of microtomed samples of developed spherulites[1,6,14,15] and quenched developing spherulites[5,11,12] revealed by electron microscopy. Also, it has been noted that the size of the symmetric eyes at the center of the spherulite grows with time. The growth of the eyes is arrested upon contact with the "edge-on" lamellae surrounding them (see Figure 8g−l). Furthermore, our observation reveals that the periphery of the developing spherulites is not as smooth as that observed by optical microscopy. It looks like a "hedgehog". The lamellar stack develops into a spherulitic shape only near the end of the growth, as shown in Figure 8j−l.

The growth rate of the spherulite and the height of the eyes measured with respect to the surrounding area are determined by using AFM at 25 ± 1 °C. The results are shown in Figure 9. The size of the spherulite increases linearly with time, suggesting that the overall growth rate of the spherulites is almost constant as observed with optical microscopy. The height of the eyes increases linearly with time until it reaches a certain point. These results indicate that the lamellar growth in the center area of the spherulites is not a two-dimensional growth even through the thickness of the BA-C8 thin film is only approximately 300 nm. The slow growth rate of the eyes may be due to the limited supply of the materials in the thin films. Detailed information on the formation of symmetric eyes around the center of the spherulites will be discussed in a forthcoming paper.

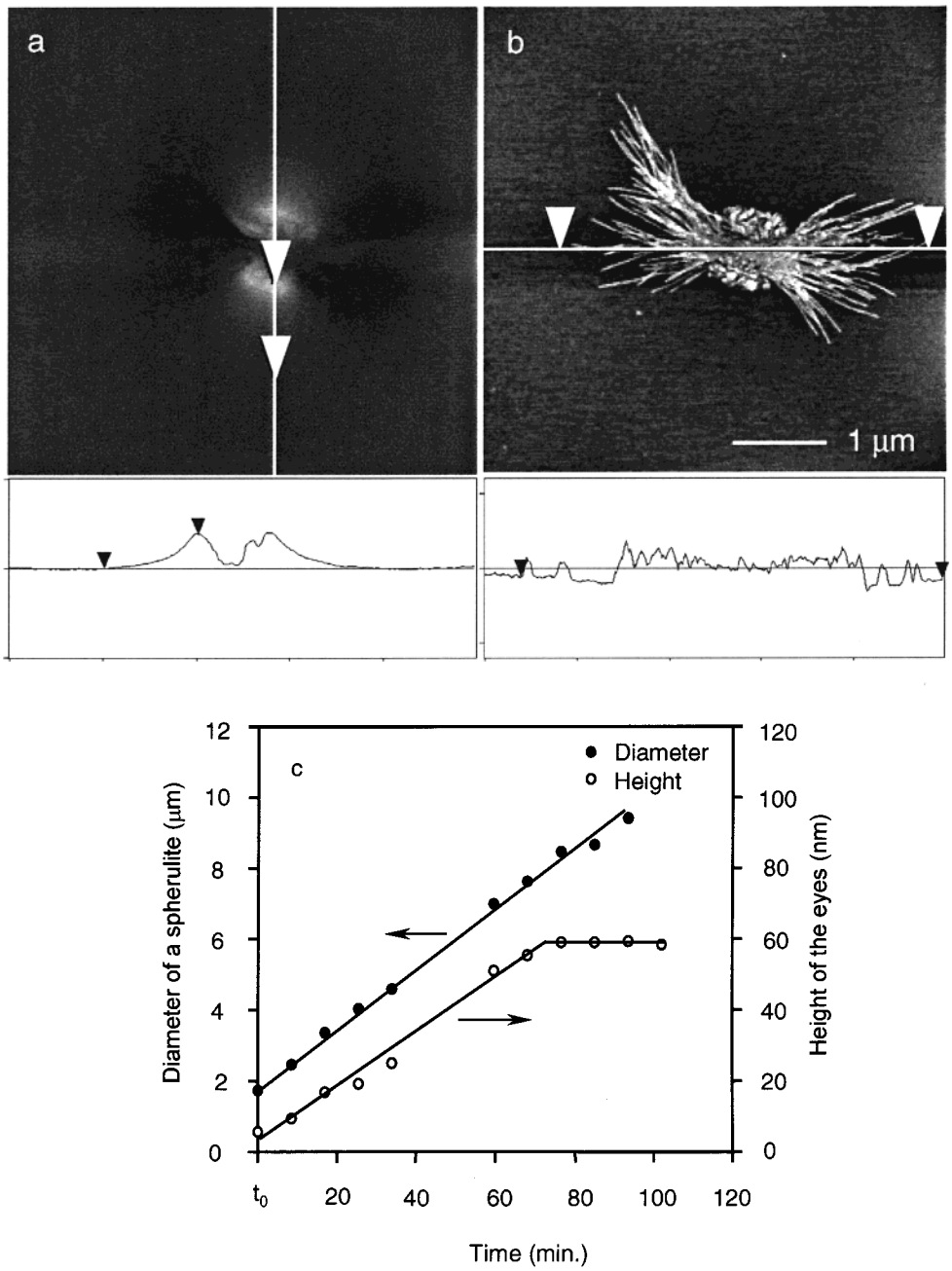

Figure 9. Height of an eye and the diameter of a spherulite measured using AFM: (a) the height of the eye; (b) the diameter of the spherulite; and (c) variation with time.

Conclusion

The direct observation of the isothermal crystallization process of the BA-C8 polymer thin film presents some important scientific information. A summary of the key experimental observations is given below.

(1) The orientation of chain segments at the tip of a growing lamella is not as perfect as the orientation of the developed regions of a lamella.

(2) The growth direction of a lamella can be changed using the AFM probe. The "*a*−*b*" plane of a lamella is more stable at a higher load from the AFM probe than the "*a*−*c*" plane.

(3) Secondary nuclei are formed by the loose loops or protruding cilia of the chain segments that are trapped in the lattice of the parent lamellae.

(4) The branching of the parent lamellae is induced by the growth of the secondary nuclei into secondary lamellae.

(5) The meeting of two growing lamellae does not necessarily terminate their growth; they may separate and continue to grow and propagate.

(6) The bending of a lamella can be induced by the stress of the chain segments that are trapped among the lamellae.

Acknowledgment. This work was supported by the Hong Kong Government Research Grant Council under Grant HKUST 9123/97P.

References and Notes

(1) Bassett, D. C. *Principles of Polymer Morphology*; Cambridge University Press: New York, 1981.

(2) Woodward, A. E. *Atlas of Polymer Morphology;* Hanser Publisher: New York, 1988.

(3) Sperling, L. H. *Introduction to Physical Polymer Science*; John Wiley and Sons: New York, 1992.

(4) Strobl, G. R. *The Physics of Polymers;* Springer-Verlag: Berlin, 1996.
(5) Bassett, D. C.; Olley, R. H. *Polymer* **1984,** *25,* 935.
(6) Norton, D. R.; Keller, A. *Polymer* **1985**, *26*, 704.
(7) Keller, A. *J. Polym. Sci.* **1955**, *17*, 291.
(8) Keith, H. D.; Padden, Jr., F. J. *J. Polym. Sci.* **1959**, *39*, 101.
(9) Keller, A.; Sawada, S. *Makromol. Chem.* **1964**, *74*, 190.
(10) Bassett, D. C.; Hodge, A. M.; Olley, R. H. *Proc. R. Soc. London* **1981**, *A377*, 25, 39, 61.
(11) Bassett, D. C.; Vaughan, A. S. *Polymer* **1985**, *26*, 717.
(12) Olley, R. H.; Bassett, D. C. *Polymer* **1989**, *30*, 399.
(13) Bassett, D. C. *Philos. Trans. R. Soc. London* **1994**, *A348*, 29.
(14) Li, J. X.; Ness, J. N.; Cheung, W. L. *J. Appl. Polym. Sci.* **1996**, *59*, 1733.
(15) Li, J. X.; Cheung, W. L. *J. Appl. Polym. Sci.* **1999**, *72*, 1529.
(16) Terrill, N. J.; Fairclough, P. A.; Ryan, A. J. *Polymer* **1998**, 2381.
(17) Akpalu, Y.; Kielhorn, L.; Hsiao, B. S. *Macromolecules* **1999**, *32*, 765.
(18) Keith, H. D.; Padden, F. J. *J. Appl. Phys.* **1963**, *34*, 2409.
(19) Miles, J. M. *Science* **1997,** *277,* 1845.
(20) Magonov, S. N. *Appl. Spectrosc. Rev.* **1993**, *28*, 1.
(21) Rugar, D.; Hansma, P. *Phys. Today* **1990**, October, 23.
(22) Magonov, S. N.; Reneker, D. *Annu. Rev. Mater. Sci.* **1997**, *27*, 175.
(23) Zhong, Q.; Innis, D.; Kjoller, K.; Elings, V. B. *Surf. Sci.* **1993**, *290*, l688.
(24) Magonov, S. N.; Elings, V.; Whangbo, M.-H. *Surf. Sci.* **1997**, *375*, L385.
(25) Bar, G.; Thomann, Y.; Brandsch, R.; Cantow, H.-J.; Whangbo, M.-H. *Langmuir* **1997**, *13*, 3807.
(26) Bar, G.; Delineau, L.; Brandsch, R.; Bruch, M. H.-J.; Whangbo, M.-H. *Appl. Phys. Lett.* **1999**, *75*, 4198.
(27) Bar, G.; Brandsch, R. H.-J.; Whangbo, M.-H. *Surf. Sci.* **1999**, *436*, L715.
(28) Magonov, S.; Godovsky, Y. *Am. Lab.* **1999**, *31* (April), 52.
(29) Höper, R.; Gesang, T.; Possart, W.; Hennemann, Boseck, S. *Ultramicroscopy* **1995**, *60*, 17.
(30) Magonov, S. N.; Cleveland, J.; Elings, V.; Denley, D.; Whangbo, M.-H. *Surf. Sci.* **1997**, *389*, 201.
(31) Leclère, Ph.; Lazzaroni, R.; Brédas, J. L. *Langmuir* **1996**, *12*, 4317.
(32) Patil, R.; Kim. S.-J.; Smith, E.; Reneker, D. H.; Weisenhorn, A. L. *Polym. Commun.* **1990**, *31*, 455.
(33) Snetivy, D.; Vancso, G. J. *Polymer* **1992**, *33*, 432.
(34) Pearce, R.; Vancso, G. J. *Polymer* **1998**, *39*, 1237.
(35) Pearce, R.; Vancso, G. J. *J. Polym. Sci., Polym. Phys.* **1998**, *36*, 2643.
(36) Haeringen, D. T.-V.; Varga, J.; Ehrenstein, G. W.; Vancso, G. J. *J. Polym. Sci., Polym. Phys.* **2000**, *38*, 672.
(37) Harbon, H. R.; Pritchard, R. G.; Cope, B. C.; Goddard, D. T. *J. Polym. Sci., Polym. Phys.* **1996**, *34*, 173.
(38) Crämer, K.; Wawkuschewski, A.; Domb, A.; Cantow, H.-J.; Magonov, *Polym. Bull.* **1995**, *35*, 457.
(39) Motomatsu, M.; Nie, H.-Y.; Mizutani, W.; Tokumoto, *Polym. Commun.* **1996**, *37*, 183.
(40) Ivanov, D. A.; Jonas, A. M. *Macromolecules* **1998**, *31*, 4546.
(41) Trifonova, D.; Varga, J.; Vancso, G. J. *Polym. Bull.* **1998**, *41*, 341.
(42) Godovsky, Y. K.; Magonov *Langmuir* **2000**, *16*, 3549.
(43) Bartczak, Z.; Argon, A. S.; Cohen, R. E.; Kowalewski, T. *Polymer* **1999**, *40*, 2367.
(44) Schultz, J. M.; Miles, M. J. *J. Polym. Sci., Polym. Phys.* **1998**, *36*, 2311.
(45) Hobbs, J. K.; McMaster, T. J.; Miles, M. J.; Barham, P. J. *Polymer* **1998**, *39*, 2437.
(46) Li, L.; Chan, C.-M.; Li, J. X.; Ng, K. M.; Yeung, K. L.; Weng, L. T. *Macromolecules* **1999**, *32*, 8240.
(47) Li, L.; Ng, K. M.; Chan, C.-M.; Feng, J.; Zeng, X.-M.; Weng, L. T. *Macromolecules* **2000**, *33*, 5588.
(48) Schonherr, H.; Snetivy, D.; Vancso, G. J. *Polym. Bull.* **1993**, *30*, 567.
(49) Rench, G. J.; Phillips, P. J.; Vatansever, N. J. *Polym. Sci., Polym. Phys.* **1986**, *24*, 1943.
(50) Li, L. Ph.D. Thesis, Hong Kong University of Science and Technology, 1999.
(51) Strobl, G. *Eur. Phys. J. E* **2000**, *3*, 165.
(52) Flory, P. J.; Yoon, D. Y. *Nature* **1978**, 226.

MA000273E